FULL PAPER

ADVANCED FUNCTIONAL MATERIALS

DOI: 10.1002/adfm.200700051

Low-Work-Function Surface Formed by Solution-Processed and Thermally Deposited Nanoscale Layers of Cesium Carbonate**

By *Jinsong Huang*, *Zheng Xu*, and *Yang Yang**

Nanostructured layers of Cs_2CO_3 are shown to function very effectively as cathodes in organic electronic devices because of their good electron-injection capabilities. Here, we report a comprehensive study of the origin of the low work function of nanostructured layers of Cs_2CO_3 prepared by solution deposition and thermal evaporation. The nanoscale Cs_2CO_3 layers are probed by various characterization methods including current–voltage (*I–V*) measurements, photovoltaic studies, X-ray photoelectron spectroscopy (XPS), UV photoelectron spectroscopy (UPS), and impedance spectroscopy. It is found that thermally evaporated Cs_2CO_3 decomposes into CsO_2 and cesium suboxides. The cesium suboxides dope CsO_2, yielding a heavily doped n-type semiconductor with an intrinsically low work function. As a result, devices fabricated using thermally evaporated Cs_2CO_3 are relatively insensitive to the choice of the cathode metal. The reaction of thermally evaporated Cs_2CO_3 with Al can further reduce the work function to 2.1 eV by forming an Al–O–Cs complex. Solution-processed Cs_2CO_3 also reduces the work function of Au substrates from 5.1 to 3.5 eV. However, devices prepared using solution-processed Cs_2CO_3 exhibit high efficiency only if a reactive metal such as Al or Ca is used as the cathode metal. A strong chemical reaction occurs between spin-coated Cs_2CO_3 and thermally evaporated Al. An Al–O—Cs complex is formed as a result of this chemical reaction at the interface, and this layer significantly reduces the work function of the cathode. Finally, impedance spectroscopy results prove that this layer is highly conductive.

1. Introduction

The nanometer-sized interfacial layer between the metal cathode and the organic semiconductor plays a critical role in controlling the performance of organic light-emitting devices (OLEDs).[1–14] Cs_2CO_3 has been shown to be a very efficient electron-injection material in OLEDs, including in OLEDs based on small molecules[9,11] and polymers (polymer light-emitting diodes (PLEDs)).[10,14] It has been shown that there is a three-fold increase in the efficiency of a white-light-emitting PLED upon the insertion of a thin Cs_2CO_3 layer between the light-emitting polymer (LEP) and the Al cathode.[10] It is also known that Cs_2CO_3 is more effective than LiF in terms of facilitating electron injection, because devices using a Cs_2CO_3 electron-injection layer have a lower driving voltage, and hence exhibit a higher power efficiency. In addition, more materials can be used as the cathode metal when Cs_2CO_3 is used as the electron-injection layer. Furthermore, the electron-injection ability of the interfacial layer can be precisely controlled by adjusting the thickness of Cs_2CO_3, and thus balanced electron and hole currents can be achieved to realize optimal device performance.[14] Owing to the above reasons, Cs_2CO_3 has been increasingly used in organic electronic devices. For example, it has been used as the connecting unit in tandem OLED cells,[12] as an electrode material in inverted photovoltaic devices,[13] and as a dopant for other electron-transport materials.[9,11] Notably, Cs_2CO_3 can be processed either by thermal evaporation[9,11,12,14] or spin-coating.[10,13] Cs_2CO_3 has a high solubility in polar solvents such as water and alcohol, and is almost completely insoluble in most other organic solvents such as toluene, *p*-xylene, and chlorobenzene. Thus, the deposition of Cs_2CO_3 layers is compatible with the solution processing of multilayer PLED structures. Furthermore, once all the device parameters have been optimized, there is no obvious difference in device efficiency using these two processes. This point is discussed in more detail below.

However, in contrast to well-known LiF, it is still not clear how Cs_2CO_3 works in improving electron injection. Here, we report a systematic study of the origin of the good electron-injection capabilities of Cs_2CO_3 layers fabricated by solution processing or thermal deposition. The electron-injection capabilities of Cs_2CO_3 layers have been studied using PLEDs with cathodes fabricated from several different metals. The devices have been first characterized by current–voltage (*I–V*) measurements to demonstrate increased electron injection by Cs_2CO_3. Secondly, the increased electron injection is explored

[*] Prof. Y. Yang, J. Huang, Z. Xu
Department of Materials Science and Engineering
University of California Los Angeles
Los Angeles, CA 90095 (USA)
E-mail: yangy@ucla.edu

[**] J. Huang and Z. Xu contributed equally to this work. We wish to thank Dr. Kazunori Ueno, Dr. Sven Andresen, and Dr. Satoru Shiobara from Canon Inc. for their comments and discussion. Financial support from Canon Inc. in Japan is acknowledged.

ADVANCED FUNCTIONAL MATERIALS

by measuring the change of the cathode work function in real devices. This is achieved by studying the built-in potential of the devices by photovoltaic measurements. The interface electronic structure and variations in the work function have been further examined by X-ray photoelectron spectroscopy (XPS) and UV photoelectron spectroscopy (UPS). The analysis of high-performance devices fabricated using Cs/Al cathodes corroborates the results obtained by other techniques. Finally, impedance spectroscopy results show that ohmic contacts are formed at the Cs_2CO_3 interface.

2. Results and Discussion

2.1. *I–V* Characteristics

In order to determine how the electron-injection layer forms and functions, PLEDs have been fabricated with various Cs_2CO_3 thicknesses by thermal evaporation. For comparison, PLEDs have also been fabricated using solution-processed Cs_2CO_3. All the devices have the structure indium tin oxide (ITO)/ poly(3,4-ethylenedioxythiophene) (PEDOT)/LEP/ Cs_2CO_3/Al (or Ag), where the LEP is a blend of polyfluorene (PF) and poly(2-methoxy-5-(2′-ethylhexoxy)-1,4-phenylenevinylene) (MEH-PPV). In order to verify if Al must be used as the metal cathode to achieve high performance, devices have also been fabricated using Ag as the cathode. Ag is chosen because it has a work function similar to that of Al, but is much less chemically reactive. The thickness of the thermally evaporated Cs_2CO_3 is varied from 0.3 to 30 Å. The thickness of the solution-processed Cs_2CO_3 is estimated by XPS absorption to be about 20 Å. Here, the notation Cs_2CO_3 (sol)/Al, Cs_2CO_3 (sol)/Ag, Cs_2CO_3 (evp)/Al, and Cs_2CO_3 (evp)/Ag denote devices with solution-processed Cs_2CO_3/Al, solution-processed Cs_2CO_3/Ag, thermally evaporated Cs_2CO_3/Al, and thermally evaporated Cs_2CO_3/Ag cathodes, respectively. The notations Cs_2CO_3 (evp) and Cs_2CO_3 (sol) are used to denote thermally evaporated and solution-processed Cs_2CO_3, respectively, because the thermally evaporated Cs_2CO_3 is indeed no longer Cs_2CO_3 on the substrate, as discussed in the subsequent sections.

2.1.1. Thermally Evaporated Cs_2CO_3

Figure 1 shows *I–V* plots for Cs_2CO_3 (evp)/Al and Cs_2CO_3 (evp)/Ag devices with the Cs_2CO_3 thickness varying from 0.3 to 30 Å. Figure 1 clearly shows that the current increases with increasing Cs_2CO_3 thickness for both the Al and Ag cathodes. For the thicknesses tested here, no decrease in current is observed for thick Cs_2CO_3 films. In contrast to the results of Hasegawa et al.,[9] we have observed some small but clear differences between Cs_2CO_3 (evp)/Al and Cs_2CO_3 (evp)/Ag devices in terms of the magnitude of the injected current. For devices with the same parameters, Cs_2CO_3 (evp)/Al devices exhibit higher currents than their Cs_2CO_3 (evp)/Ag counterparts. Since the work functions of Al and Ag are very similar, the difference in device current is ascribed to their different

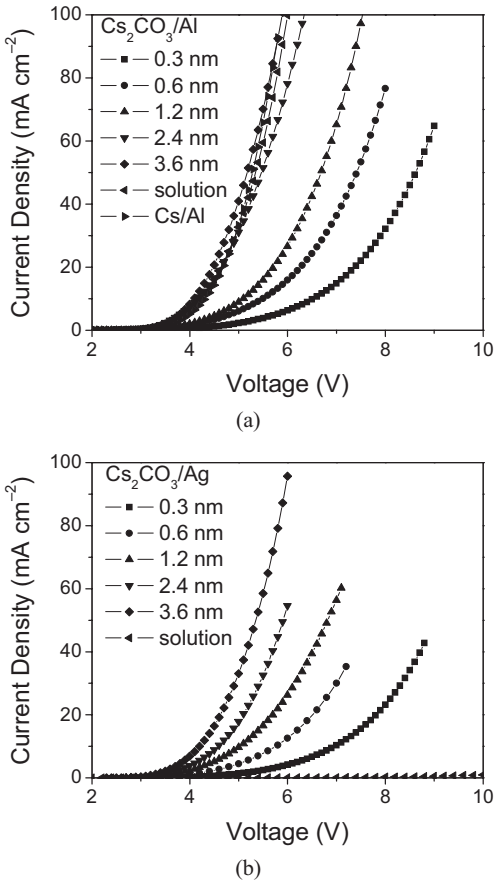

Figure 1. *I–V* curves of devices with different Cs_2CO_3 (thermally deposited) thicknesses using a) Al and b) Ag as the cathode metals; the *I–V* curves of devices based on solution-processed Cs_2CO_3 are also shown in each panel. The *I–V* curve of the Cs/Al device is shown in (a).

chemical reactivity. The interfacial layer formed by the reaction of Al with thermally evaporated Cs_2CO_3 is able to further increase the electron injection, as also suggested by the XPS/UPS measurements discussed in subsequent sections. One problem with Cs_2CO_3 (evp)/Ag devices is that they are easily electrically shorted, likely due to the diffusion of Ag into the LEP layer. Unfortunately, the morphology of the deposited film is difficult to characterize by atomic force microscopy (AFM) under an ambient atmosphere because the surface tends to absorb moisture rapidly.

2.1.2. Solution-Processed Cs_2CO_3

Figure 1 also shows the *I–V* curves of Cs_2CO_3 (sol)/Al and Cs_2CO_3 (sol)/Ag devices. The current observed for the Cs_2CO_3 (sol)/Al device is comparable to that of the device with 24 Å of thermally evaporated Cs_2CO_3. This result is reasonable because the thickness of the solution-deposited Cs_2CO_3 is around 20 Å. In contrast, the current observed for the Cs_2CO_3 (sol)/Ag device is as small as that for a device with only an Al cathode. This result suggests that solution-processed Cs_2CO_3 does not play a significant role in increasing the injection of

electrons from Ag. Again the large observed difference is ascribed to the different chemical reactivities of the two metals. We conclude that the reaction of Al with spin-coated Cs_2CO_3 is important to obtain an interface optimal for electron injection. Another conclusion that can be drawn from this data is that the idea of doping of the LEP by Cs_2CO_3 can be rejected as the main reason for increased electron injection. Indeed, this is very different from the situation of Cs_2CO_3 doped into tris(8-hydroxyquinoline) aluminum (Alq_3).[12] If the polymer layer were to be doped by Cs_2CO_3 (sol), a thin n-type region would be formed at the LEP/cathode interface, and there would not be such a huge difference in current injection between Cs_2CO_3 (sol)/Ag and Cs_2CO_3 (sol)/Al devices.

2.2. Built-in Potential from Photovoltaic Measurements

In order to better understand the mechanism responsible for the increased electron injection from Cs_2CO_3 (evp), the work function of the Cs_2CO_3 (evp)/Al cathode has been evaluated by photovoltaic measurements. Analogous to electro-absorption measurements,[15] photovoltaic measurements provide information about the work function shift of an electrode when there is no internal charge transfer.[16,17] In this measurement, the photoinduced current is measured after subjecting the devices to illumination from a 1.5 M global solar simulator. In order to exclude the effect of the leakage current, the dark current is subtracted from the photocurrent to obtain the modified *I–V* curve. The open-circuit voltage (V_{OC}) is obtained from the modified *I–V* curve (the voltage when the current is zero). The V_{OC} deduced from photovoltaic measurements reflects the built-in potential in the PLED devices. In the absence of an interfacial dipole, the built-in potential is the difference between the work functions of the anode and the cathode in PLED devices. Since all the parameters are the same in our devices except for the thickness of Cs_2CO_3 (evp), the dipole configuration (if any) at the interface is assumed to be the same in all the devices. Thus, the shift in V_{OC} should scale with the change in the work function of the cathode. Figure 2 shows the relationship of the measured V_{OC} with the thickness of Cs_2CO_3 (evp) for both the Al and Ag cathodes. It is clear that the V_{OC} increases with the thickness of Cs_2CO_3 (evp) up to a maximum value for both the Al or Ag cathodes, and then saturates upon the formation of bulk Cs_2CO_3 (evp). As mentioned above, higher V_{OC} values essentially indicate lower work functions for the Cs_2CO_3 (evp)/Al cathodes. The photovoltaic measurements provide direct evidence that evaporated Cs_2CO_3 can reduce the work function of Al and Ag, thereby increasing electron injection. It has been reported that the low work function of thermally evaporated Cs_2CO_3 is an intrinsic property of the material.[18,19] Therefore, the observed evolution of the work function with varying Cs_2CO_3 thicknesses demonstrates the extent to which the evaporated Cs_2CO_3 covers the surface.

It is worth noting that the saturated V_{OC} of Cs_2CO_3 (evp)/Ag devices is smaller than that of Cs_2CO_3 (evp)/Al devices, which means that even lower work functions can be achieved for the Cs_2CO_3 (evp)/Al cathodes. This is also consistent with the *I–V* results shown in Figure 1. The power efficiencies of these devices at a luminance of 100 cd cm^{-2} are also plotted in Figure 2a. The power efficiency follows the same trend as V_{OC} when the Cs_2CO_3 (evp) thickness is less than 15 Å. However, it quickly reaches a maximum at a Cs_2CO_3 (evp) thickness of 15 Å and then decreases as the Cs_2CO_3 (evp) thickness is further increased. It is reasonable that the power efficiency increases with increased Cs_2CO_3 (evp) thickness since electron injection becomes easier in the device. However, when the electron injection is too strong, the electron current in the LEP layer overrides the hole current, and thus the efficiency decreases with increasing Cs_2CO_3 (evp) thickness due to imbalanced charges.

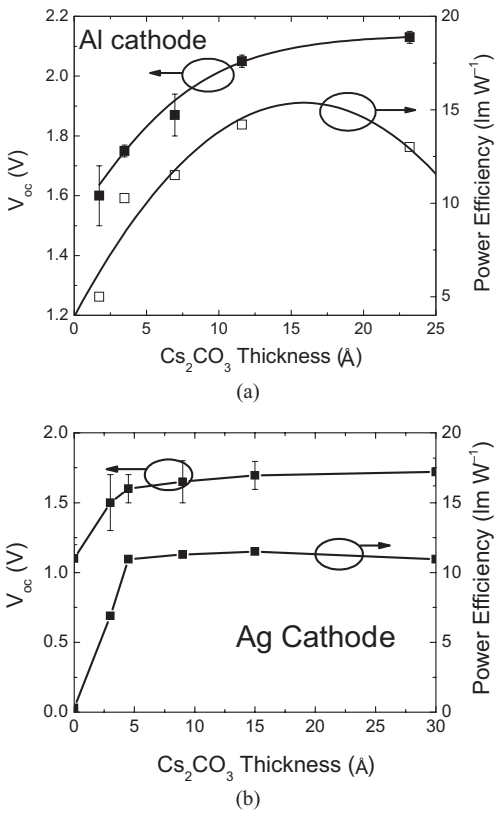

Figure 2. Open-circuit voltage of devices with different Cs_2CO_3 (thermally deposited) thicknesses using a) Al and b) Ag as the cathode metals.

The V_{OC} of the Cs_2CO_3 (sol)/Al device coincides with the saturated V_{OC} of Cs_2CO_3 (evp)/Al devices. Again, we find that the maximum power efficiency of the Cs_2CO_3 (sol)/Al device is the same as that for Cs_2CO_3 (evp)/Al devices when the device parameters are optimized. This is not surprising given that a similar complex, Al–O–Cs, is formed at the Cs_2CO_3 (sol and evp)/Al interface, leading to the observed performance enhancement in both types of devices.

2.3. XPS and UPS Studies of the Interface

To further understand the mechanism for enhanced electron injection at the atomic scale, the interface between Al and Cs_2CO_3 (sol and evp) has been studied by XPS and UPS. Thermally evaporated Cs_2CO_3 tends to decompose into CsO_2 and

ADVANCED FUNCTIONAL MATERIALS

CO_2. In contrast, solution-processed Cs_2CO_3 is not as prone to decomposition. Therefore, understanding the fundamental mechanism underlying the enhanced electron injection is critical for achieving reproducible device performance.

2.3.1. Thermally Evaporated Cs_2CO_3

Thermally evaporated Cs_2CO_3 has been used to produce low-work-function surfaces.[18,19] A low work function of around 1 eV has been achieved by Cs_2CO_3 decomposition followed by careful high-temperature annealing at 550–600 °C. In contrast to studies of the thermionic emission of hot electrons, we have studied the decomposition of the Cs_2CO_3 cathode for electron injection into the organic material. It has previously been suggested that Cs_2CO_3 decomposes into stoichiometric CsO_2 doped with Cs_2O_2 during thermal evaporation; the doped oxide behaves as a kind of n-type semiconductor with an estimated bandgap of 1.9 eV.[19,20] Nevertheless, this hypothesis has not been proven by experimental data and Cs_2O_2 has not been conclusively identified. We have observed the evolution of CO_2 by mass spectrometry during the evaporation of Cs_2CO_3 under a high vacuum, which suggests that Cs_2CO_3 decomposes under our experimental conditions. However, the Cs:O atomic ratio in the thermally evaporated films, as derived by integrating the XPS signal intensities, is 2.096. Therefore, clearly the thermally deposited film contains cesium suboxides (e.g., Cs_7O, Cs_4O, Cs_3O, and Cs_7O_2) doped into the CsO_2 or Cs-doped CsO_2, rather than Cs_2O_2, under our experimental conditions. The obtained film behaves as a heavily doped n-type semiconductor.[19,20] It is worth noting that Wu et al.[11] have observed a signal from C in their thermally deposited films, which might originate from the incomplete decomposition of Cs_2CO_3 during thermal evaporation under the experimental conditions used. Alternatively, it is also possible that this signal arises from organic contaminants desorbed from the inner wall of the vacuum chamber.

A Ag substrate has been prepared by depositing a thin layer of Ag metal on a Si wafer. The Ag substrate is subjected to Ar sputtering to remove molecules adsorbed from air before Cs_2CO_3 deposition. After depositing 16 Å of Cs_2CO_3 (evp) onto the substrate, 16 Å of Al is also deposited on the surface. XPS and UPS spectra have been measured after the deposition of each layer. Figure 3 shows the UPS spectra at a) the secondary electron cut-off and b) near the Fermi edge. There is a large shift (2.1 eV) of the secondary electron cut-off towards lower binding energies after Cs_2CO_3 deposition, which suggests that the work function of the Ag substrate surface is lowered by 2.1 eV. Here, we feel that it is better to adopt the term "effective work function" to describe the properties of this surface, because thermally evaporated Cs_2CO_3 (which is predominantly CsO_2) is not a metal. Although some have argued that Cs_2O-covered surfaces exhibit metallic behavior,[21] we have not observed a clear Fermi edge in our experiments. In the past, the term "effective work function" has been used to describe the thermionic emission cathode.[19] The effective work function of our deposited CsO_2 surface is calculated to be 2.2 eV. In order to test if this work function is an intrinsic property of the material (i.e., a property of the bulk material), we have deposited 80 Å Cs_2CO_3 on Au. A 16 Å film of thermally evaporated Cs_2CO_3 has a work function of 2.2 eV; the work function slowly decreases to 2.0 eV when the thickness of the deposited Cs_2CO_3 is increased to 80 Å. All these results illustrate that the observed low work function of thermally evaporated Cs_2CO_3 (cesium suboxide) is an intrinsic property, and not just a surface phenomenon. Therefore, this low-work-function film is not very sensitive to the substrate used, which explains why metals such as Al, Au, and Ag can be used as cathodes in OLEDs with a similar device performance.[9] We also note that the effective work function measured here is about 1 eV higher than the value reported previously in the literature.[19] One possible reason for this is that our thermally evaporated Cs_2CO_3 film has not been thermally annealed at a very high temperature. Fortunately, this work function is still low enough to ensure the injection of electrons into most organic materials, as long as there is no additional dipole formation at the interface to increase the electron-injection barrier.

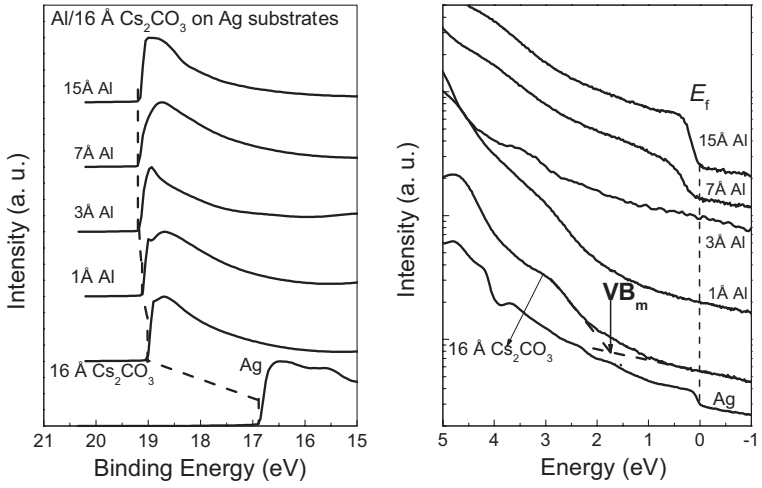

Figure 3. UPS spectra around a) the secondary electron cut-off, and b) the Fermi energy for a 16 Å thermally deposited film of Cs_2CO_3 before and after the deposition of Al layers with thicknesses ranging from 1 to 15 Å.

There is a small decrease in the work function (by about 0.16 eV) upon the deposition of 3 Å Al on the prepared CsO_2 layer. The work function does not decrease any further when the thickness of Al is increased beyond 3 Å. Considering that the lattice constant of Al is 3 Å, this corresponds to a monolayer of Al atoms. XPS measurements reveal that this monolayer of Al exists in the form of an oxide. Therefore, the results suggest that the first monolayer of Al reacts with CsO_2, thereby further decreasing the work function. Since O atoms are simultaneously bonded to both Cs and Al atoms, it is believed that an Al–O–Cs complex is formed in this monolayer; this interfacial complex has an even lower work function than decomposed Cs_2CO_3. Indeed, it is well known that the formation of element–O–Cs structures is essential for obtaining a low-work-

function (or negative-work-function) surface, as seen for C–O–Cs,[22] W–O–Cs,[23] Si–O–Cs,[24] Ga–O–Cs,[25] etc. It seems that CsO_2 does not react very well with Ag due to the low chemical reactivity of the latter, which might explain the relatively lower efficiency of Ag cathodes as compared to their Al counterparts. Nakamura et al. have found that the oxidation of Cs at the Cs/Al interface is responsible for enhanced electron injection, and oxidized Cs/Ag cathodes are less effective than oxidized Cs/Al cathodes in improving device efficiency.[26]

Figure 3b shows the UPS spectra around the Fermi edge. The spectra are vertically shifted and plotted on a logarithmic scale to clearly display the Fermi edge. No Fermi edge is observed for thermally deposited Cs_2CO_3, which implies that thermally deposited Cs_2CO_3 is a semiconductor rather than a metal. The Fermi edge becomes clearly visible only after Cs_2CO_3 is covered by 7 Å of Al, which again proves that the first monolayer of Al reacts with Cs_2CO_3 (evp). The valence band of the deposited Cs_2CO_3 can be identified and the valence-band maximum (VB_m) is extracted as shown in the figure. The VB_m is about 1.8 eV below the Fermi energy, which is very close to the band-gap of CsO_2 (1.9 eV). Therefore, the thermally evaporated Cs_2CO_3 indeed behaves as a heavily n-doped semiconductor exhibiting high conductivity. To the best of our knowledge, this is the first time that such an energy structure has been experimentally observed. This explains the high power efficiency of devices using Cs_2CO_3 (evp) as the electron-injection layer, since owing to its high conductivity there is no voltage drop across this layer. Based on these observations, the energy diagram between Al and the deposited Cs_2CO_3 is shown in Figure 4. As clearly depicted in Figure 4, the work function of Al is 4.3 eV, whereas the deposited Cs_2CO_3 surface has a low work function of 2.2 eV due to the large displacement from the vacuum level by 2.1 eV. More importantly, there is no barrier for the injection of electrons from Al to the conduction band of the highly conductive n-type Cs_2CO_3 (evp) semiconductor.

The formation of an Al–O–Cs complex at the contact between Al and Cs_2CO_3 (evp) slightly lowers the bulk work function of Cs_2CO_3; the formation of this complex also contributes to a small increase in the device efficiency of PLEDs fabricated using a thermally evaporated Cs_2CO_3 interfacial layer. However, this mechanism is much more important in solution-processed Cs_2CO_3 devices.

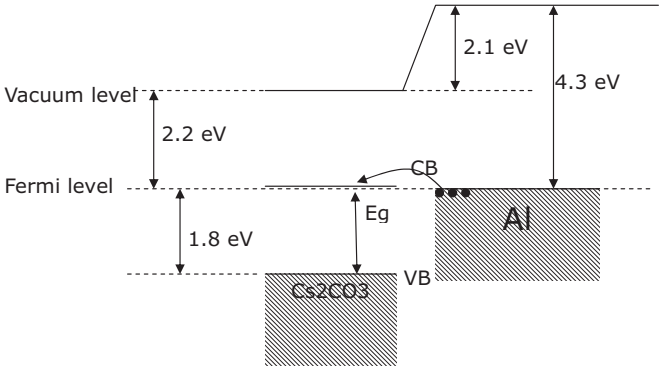

Figure 4. Energy structure of the thermally deposited Cs_2CO_3/Al interface.

2.3.2. Solution-Processed Cs_2CO_3

Devices with spin-coated Cs_2CO_3 exhibit performance comparable to the best (or optimized) devices containing thermally evaporated Cs_2CO_3. At first glance it is surprising that devices with spin-coated Cs_2CO_3 should work so well, because spin-coated Cs_2CO_3 is unable to decompose into low-work-function CsO_2. The doping of the polymer by Cs_2CO_3 (sol) is also unlikely in our system, because the device performance is poor when Ag is used as the cathode metal. Therefore, we believe that the reaction between Cs_2CO_3 (sol) and the evaporated metal plays a critical role in decreasing the work function.

The reaction of Cs_2CO_3 (sol) with evaporated Al has been demonstrated by XPS. Figure 5 shows spectra corresponding to the O 1s and Al2s core levels. After deposition of the first 2 Å of Al, the XPS measurements indicate the presence of only the oxide. As mentioned above, this thickness corresponds to only

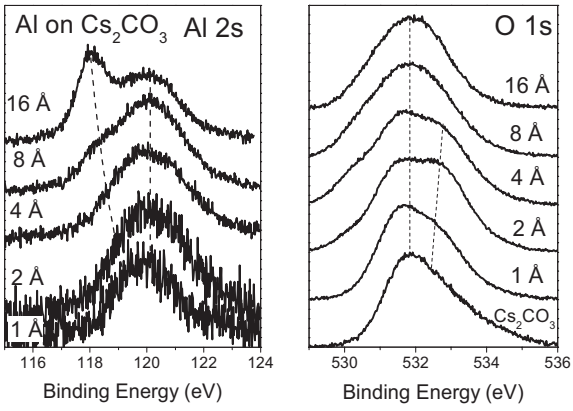

Figure 5. XPS spectra of solution-processed Cs_2CO_3 before and after the deposition of Al layers with thicknesses ranging from 0.5 to 16 Å.

about a monolayer of Al atoms. The first layer of Al atoms form strong chemical bonds with the underlying Cs_2CO_3 (sol) layer. Metallic Al only begins to appear after the deposition of a second layer of Al atoms. For solution-processed Cs_2CO_3, the O 1s emission is characterized by a single very broad peak. Another peak is observed upon the deposition of Al onto Cs_2CO_3 (sol), which is attributed to the formation of an O–Al bond. Undoubtedly, there are many O atoms bonded to both Al and Cs in the Al–O–Cs structure. This interfacial layer thus plays a very critical role in reducing the work function of the cathode.

The UPS results for Al thin films deposited on solution-processed Cs_2CO_3 are shown in Figure 6. A layer of Ag coated on a Si substrate serves as a reference; subsequently, a thin layer of Cs_2CO_3 is spin-coated onto the Ag layer. As clearly apparent from Figure 6a, the work function of the Ag surface decreases by 0.8 eV after it is covered by Cs_2CO_3. The work function of the spin-coated Cs_2CO_3 surface is calculated to be 3.5 eV. These are the first measurements of the work function of nanostructured Cs_2CO_3 thin films on substrates. This data explains why high-work-function ITO can be used as a cathode after spin-coating a thin layer of Cs_2CO_3 (sol) on it.[13] The

ADVANCED FUNCTIONAL MATERIALS

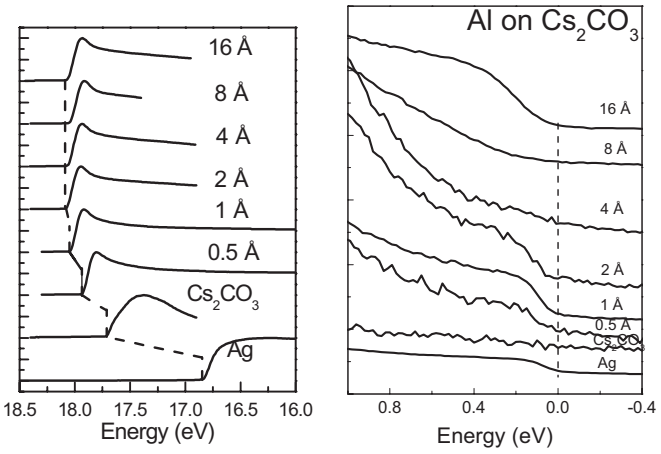

Figure 6. UPS spectra of solution-processed Cs_2CO_3 before and after the deposition of Al with thicknesses ranging from 0.5 to 16 Å. Si coated with Ag is used as the substrate.

work function of the Cs_2CO_3 (sol)-covered substrate is further dramatically decreased by the deposition of a thin layer of Al; the work function saturates after the coverage of Al reaches 4 Å (one monolayer of Al atoms). This saturation behavior is reasonable because the origin of the reduced work function is the reaction of Al with Cs_2CO_3 (sol) resulting in the formation of Al–O–Cs. There is almost no reaction between the second layer of Al and Cs_2CO_3 (sol), as evidenced by XPS measurements. The lowest work function obtained (saturated work function) is 2.8 eV, which is higher than that of thermally evaporated Cs_2CO_3 (2.2 eV). However, we have found that real devices fabricated by the two different processes exhibit very similar characteristics: the same order of magnitude current for the same Cs_2CO_3 thicknesses, the same maximum efficiencies, and the same saturated built-in potentials, as shown in Figure 2. One would expect that a similar work function should be obtained for Cs_2CO_3 layers fabricated by different processes, because the origin of the decreased work function is the formation of the same final product, the Al–O–Cs complex. One possible reason for this observed discrepancy is that the spin-coated Cs_2CO_3 film on Ag may not be continuous. Unlike in real devices, here there are no surfactants mixed with Cs_2CO_3 (sol). This eliminates the photoemission from C and O present in the surfactant, which would make the spectroscopic studies unclear. Nevertheless, the work function of the Al–O–Cs structure is believed to be around 2 eV.

Figure 6b shows the UPS spectra around the Fermi level. The valence band of Cs_2CO_3 (sol) is 2.3 eV below the Fermi energy. The spectra become quite featureless after Al deposition as a result of the chemical reaction. An interesting phenomenon is observed near the Fermi edge: the Fermi edge becomes clearly visible after the deposition of 1 Å of Al. This implies that the surface is metallic in nature. Similar metallic surfaces have been observed for Cs on diamond (C–O–Cs)[22] and Cs_2O/Cs_2O_2/GaAs (Ga–O–Cs).[21] However, the surface loses its metallic character after the deposition of 4 Å (one monolayer) of Al. The origins of the metallic surface at low Al coverage (1 Å) and its transitition to the nonmetallic state as the Al coverage increases are still under investigation. When the Al coverage is sufficiently thick (16 Å), the metallic Al forms at the surface again with a clear Fermi edge.

2.4. Comparison with Cs/Al Cathodes

Cs has a particularly low work function of 2.1 eV, which is ideal for electron injection in OLEDs. Cs/Al cathodes have been demonstrated to possess good electron-injection capabilities.[26,27] However, there is clearly an additional factor at work in Cs cathode devices that can not simply be explained by the low work function of Cs. Adachi and co-workers have found that Cs no longer retains its strong electron-injection capabilities when its thickness exceeds 5 nm.[27] It has been suggested that the cathodes exhibit low work function only in the presence of a mixture of Cs and Al (or a CsAl alloy), rather than Cs alone. The possibility of the oxidation of Cs after deposition has also been considered. Since Cs is extremely reactive at room temperature, it can be readily oxidized by the residual oxygen present in the deposition chamber, oxygen absorbed in the polymer film, or oxygen anions in organic molecules during the thermal deposition process. The first monolayer of thermally deposited Cs likely exists in the form of an oxide rather than the pure metal. Indeed, XPS depth profile studies by Nakamura et al. show the presence of 10 at % oxygen at the same depth as Cs.[26] In contrast, devices with Cs/Ag cathodes containing less oxygen in the interface layer are much less efficient.[26]

We have also fabricated some devices using one monolayer of Cs between the LEP layer and the Al cathode. The performance of these devices is comparable to that of solution-processed Cs_2CO_3 devices in terms of the obtained current (Fig. 1) and power efficiency.

2.5. Impedance Spectroscopy

Impedance spectroscopy is a powerful characterization technique for studying the interfacial properties of electrical devices. The complex ac impedance Z can be represented as $Z = Z' - jZ''$, where Z' is the real part and Z'' is the imaginary part of the resistance. The dielectric loss can be represented by a Cole–Cole plot $Z'' = f(Z')$. Differently charged layers in a device can be separated in the Cole–Cole plot by treating them as equivalent resistance–capacitance (RC) circuits.[28,29] Each additional layer in a device introduces an extra RC circuit to the Cole–Cole plot. In order to clarify if Cs_2CO_3 forms ohmic contacts with Al, we have used impedance spectroscopy to further characterize the Cs_2CO_3/Al interfacial layer.

It is well known that calcium acetylacetonate $(Ca(acac)_2)$[30] introduces an extra RC element at the interface between PF:poly(9,9-dioctylfluorene-*co*-benzothiadiazole) (PF:F8BT) and the Al cathode. As shown in Figure 7a, the Cole–Cole plot of this device shows a double semicircle after it is turned on (2.6–3.5 V, forward biased). The additional low-frequency semicircle appears only when $Ca(acac)_2$ is inserted between the LEP and the Al cathode. In contrast, only one semicircle is observed when Ca is used as the cathode. Therefore, the

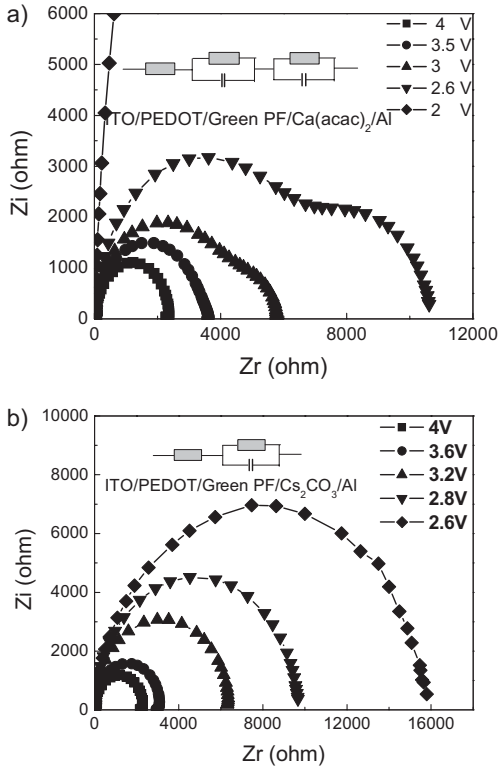

Figure 7. Cole–Cole plots of devices with a) $Ca(acac)_2$ and b) Cs_2CO_3 as the interfacial layer between the LEP (PFO + 5 % F8BT) and Al.

low-frequency semicircle must be related to the $Ca(acac)_2$ interfacial layer, whereas the semicircle at medium and high frequencies represents the response of the bulk LEP layer. The equivalent circuit of a device with $Ca(acac)_2$ is plotted in Figure 7a. The $Ca(acac)_2$ interfacial layer is believed to block holes; the accumulated holes at this layer attract electrons (due to Coulombic forces) and thus help in the injection of electrons from the cathode. In this sense, this $Ca(acac)_2$ layer has not formed an ohmic contact with Al. The resistance of $Ca(acac)_2$ as derived from the Cole–Cole plot is 480 $\Omega\,cm^2$ at 2.6 V, which is close to the bulk resistance of the LEP layer, 720 $\Omega\,cm^2$.

In comparison, only one semicircle is observed for a device containing a Cs_2CO_3 (evp and sol) interfacial layer under all forward bias conditions, as shown in Figure 7b. This means that the Cs_2CO_3 (evp and sol) layer does not act either as a resistor or a capacitor. This data implies that Cs_2CO_3 (evp and sol) reacts with Al and forms ohmic contacts, which is consistent with the results discussed in the previous sections. In terms of performance, devices with a $Ca(acac)_2$ layer have a higher driving voltage than devices with a Cs_2CO_3 (evp and sol) layer, because there is a voltage drop across the $Ca(acac)_2$ layer.

3. Conclusions and Outlook

We have studied the interfacial properties of Cs_2CO_3 layers deposited by thermal evaporation or solution processing onto Al and Ag electrodes. PLEDs fabricated using these two processes show very similar performance. Cs_2CO_3 (evp and sol) increases the electron-injection current in PLEDs by reducing the electron-injection barrier. The lowering of the work function by Cs_2CO_3 (evp and sol) is corroborated by the increased built-in potential measured in photovoltaic experiments. Thermally evaporated Cs_2CO_3 can be considered to be a heavily doped n-type semiconductor with an intrinsically low work function. This material oxidizes the first few layers of the subsequently deposited Al cathode and forms an Al–O–Cs structure, which further reduces the work function of the cathode. Solution-processed Cs_2CO_3 also chemically reacts with the deposited Al and forms a low-work-function interfacial layer. Therefore, the low work function of the cathode in devices prepared by thermal evaporation or solution processing both have the same origin: the formation of an Al–O–Cs structure at the interface.

These results provide important guidance for device design and fabrication. The observed Al–O–Cs complex can be introduced by design using other methods such as the co-evaporation of CsO_2 (or Cs_2O_2) and Al. Also, a low-work-function interface can be formed by the combination of Element A–O–Element B, where Element A is an alkali metal or alkaline earth metal and Element B is C, Si, Ga, W, Ag, etc. The compatibility with different elements permits the fabrication of stable (in terms of moisture and heat) and low-work-function cathodes.

4. Experimental

To prepare the devices, the ITO substrates were first cleaned using a routine procedure, which included sonication in detergent, repeated rinsing in deionized water, acetone, and isopropanol, and finally treatment with UV light and ozone. PEDOT:PSS (PSS: poly(styrene sulfonate), Baytron-P 4083) was spin-coated onto an ITO/glass substrate at a spinning speed of 4000 rpm, which gave a thickness of 25 nm. The PEDOT:PSS layer was baked at 150 °C for 20 min before spin-coating the LEP film. The LEP used was a mixture of PF and 5 % MEH-PPV. After spin-coating, the LEP film was baked at 70 °C for 30 min, and was then transferred to an evaporation chamber. All processes after spin-coating the PEDOT:PSS layer were performed in a glove box. The cathode of the PLED was formed by the thermal evaporation or spin-coating of Cs_2CO_3, followed by the thermal deposition of Al from tungsten boats at a pressure of around 3×10^{-6} torr (1 torr = 133 Pa).

The XPS and UPS experiments were carried out in an Omicron Nanotechnology system with a base pressure of 2×10^{-10} torr. The deposition and characterization chambers were interconnected. UPS spectra were obtained using the He I line ($h\nu = 21.2$ eV); a Mg Kα radiation source ($h\nu = 1253.6$ eV) was used for the XPS measurements. Samples were biased at –5 V during UPS measurements to observe the secondary electron edge. The Fermi energy of the system was measured before each experiment using Ag and Au substrates.

The impedance spectroscopy data was obtained at room temperature using a HP 4284A Precision LCR meter in the frequency range from 20 Hz to 1 MHz with an ac driving voltage of 30 mV. The ITO substrate was used as the positive electrode to apply a constant bias.

Received: January 12, 2007
Revised: April 18, 2007
Published online: July 12, 2007

[1] L. S. Hung, C. W. Tang, M. G. Mason, *Appl. Phys. Lett.* **1997**, *70*, 152.
[2] F. Li, H. Tang, J. Anderegg, J. Shinar, *Appl. Phys. Lett.* **1997**, *70*, 1233.

[3] Z. B. Deng, X. M. Ding, S. T. Lee, W. A. Gambling, *Appl. Phys. Lett.* **1999**, *74*, 2227.
[4] H. W. Choi, S. Y. Kim, W. K. Kim, J. L. Lee, *Appl. Phys. Lett.* **2005**, *87*, 082 102.
[5] S. A. Choulis, V.-E. Choong, M. K. Mathai, F. So, *Appl. Phys. Lett.* **2005**, *87*, 113 503.
[6] A. Chakrabarti, K. Hermann, R. Druzinic, M. Witko, F. Wagner, M. Petersen, *Phys. Rev. B: Condens. Matter* **1998**, *59*, 10 583.
[7] H. Kanno, Y. Sun, S. R. Forrest, *Appl. Phys. Lett.* **2005**, *86*, 263 502.
[8] Q. Xu, H. M. Duong, F. Wudl, Y. Yang, *Appl. Phys. Lett.* **2004**, *85*, 3357.
[9] T. Hasegawa, S. Miura, T. Moriyama, T. Kimura, I. Takaya, Y. Osato, H. Mizutani, *SID Int. Symp. Digest Technol. Papers* **2004**, *35*, 154.
[10] J. Huang, G. Li, E. Wu, Q. Xu, Y. Yang, *Adv. Mater.* **2006**, *18*, 114.
[11] C. I. Wu, C. T. Lin, Y. H. Chen, M. H. Chen, Y. J. Lu, C. C. Wu, *Appl. Phys. Lett.* **2006**, *88*, 152 104.
[12] C. W. Chen, Y.-J. Lu, C. C. Wu, E. H. Wu, C. W. Chu, Y. Yang, *Appl. Phys. Lett.* **2005**, *87*, 241 121.
[13] G. Li, C.-W. Chu, V. Shrotriya, J. Huang, Y. Yang, *Appl. Phys. Lett.* **2006**, *88*, 253 503.
[14] a) J. Huang, T. Watanabe, K. Ueno, Y. Yang, *Adv. Mater.* **2007**, *19*, 739. b) J. Huang, W. J. Hou, J. H. Li, G. Li, Y. Yang, *Appl. Phys. Lett.* **2006**, *89*, 133 509.
[15] T. M. Brown, R. H. Friend, I. S. Millard, D. J. Lacey, J. H. Burroughes, F. Cacialli, *Appl. Phys. Lett.* **2000**, *77*, 3096.
[16] G. G. Malliaras, J. R. Salem, P. J. Brock, J. C. Scott, *J. Appl. Phys.* **1998**, *84*, 1583.
[17] S. A. Choulis, V.-E. Choong, A. Patwardhan, M. K. Mathai, F. So, *Adv. Funct. Mater.* **2006**, *16*, 1075.
[18] T. R. Briere, A. H. Sommer, *J. Appl. Phys.* **1977**, *48*, 3547.
[19] A. H. Sommer, *J. Appl. Phys.* **1979**, *51*, 1254.
[20] A. Band, A. Albu-Yaron, T. Livneh, H. Cohen, Y. Feldman, L. Shimon, R. Popovitz-Biro, V. Lyahovitskaya, R. Tenne, *J. Phys. Chem. B* **2004**, *108*, 12 360.
[21] J. X. Wu, F. Q. Li, J. S. Zhu, M. R. Ji, M. S. Ma, *J. Vac. Sci. Technol. A* **2002**, *20*, 1532.
[22] W. E. Pickett, *Phys. Rev. Lett.* **1994**, *73*, 1664.
[23] J. L. Desplat, *Surf. Sci.* **1973**, *34*, 588.
[24] R. U. Martinelli, *J. Appl. Phys.* **1974**, *45*, 1183.
[25] J. D. Levine, F. E. Gelhaus, *J. Appl. Phys.* **1967**, *36*, 892.
[26] A. Nakamura, T. Tada, M. Mizukami, S. Yagyu, *Appl. Phys. Lett.* **2004**, *84*, 130.
[27] T. Oyamada, C. Maeda, H. Sasabe, C. Adachi, *Jpn. J. Appl. Phys.* **2003**, *42*, 1535.
[28] T. F. Guo, G. He, S. Pyo, Y. Yang, *Appl. Phys. Lett.* **2002**, *80*, 4042.
[29] T. van Woudenbergh, J. Wildeman, P. W. M. Blom, J. J. A. M. Bastiaansen, B. M. W. Langeveld-Vos, *Adv. Funct. Mater.* **2004**, *14*, 677.
[30] Q. Xu, J. Ouyang, Y. Yang, T. Ito, J. Kido, *Appl. Phys. Lett.* **2003**, *83*, 8.